Free-Standing Porous Carbon Nanofiber/Ultrathin Graphite Hybrid for Flexible Solid-State Supercapacitors

Kaiqiang Qin,[†,‡] Jianli Kang,[*,‡,§] Jiajun Li,[†] Chunsheng Shi,[†] Yuxiang Li,[∥] Zhijun Qiao,[∥] and Naiqin Zhao[*,†,⊥]

[†]School of Materials Science and Engineering and Tianjin Key Laboratory of Composites and Functional Materials, Tianjin University, Tianjin 300072, China, [‡]School of Materials Science and Engineering, Tianjin Polytechnic University, Tianjin 300387, China, [§]State Key Laboratory of Hollow Fiber Membrane Materials and Processes, Tianjin Polytechnic University, Tianjin 300387, China, [∥]School of Mechanical Engineering, Tianjin Polytechnic University, Tianjin 300387, China, and [⊥]Collaborative Innovation Center of Chemical Science and Engineering, Tianjin 300072, China

ABSTRACT A micrometer-thin solid-state supercapacitor (SC) was assembled using two pieces of porous carbon nanofibers/ultrathin graphite (pCNFs/G) hybrid films, which were one-step synthesized by chemical vapor deposition using copper foil supported Co catalyst. The continuously ultrathin graphite sheet (~25 nm) is mechanically compliant to support the pCNFs even after etching the copper foil and thus can work as both current collector and support directly with nearly ignorable fraction in a SC stack. The pCNFs are seamlessly grown on the graphite sheet with an ohmic contact between the pCNFs and the graphite sheet. Thus, the accumulated electrons/ions can duly transport from the pCNFs to graphite (current collector), which results in a high rate performance. The maximum energy density and power density based on the whole device are up to 2.4 mWh cm^{-3} and 23 W cm^{-3}, which are even orders higher than those of the most reported electric double-layer capacitors and pseudocapacitors. Moreover, the specific capacitance of the device has 96% retention after 5000 cycles and is nearly constant at various curvatures, suggesting its wide application potential in powering wearable/miniaturized electronics.

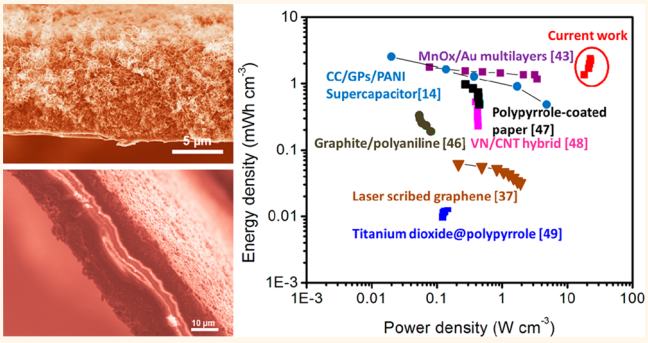

KEYWORDS: porous carbon nanofiber · ultrathin graphite · flexible solid-state supercapacitor · device performance · chemical vapor deposition

With the fast growing demand for miniaturized and wearable electronic devices, the design and fabrication of compatible energy storage devices become new challenges.[1−6] Supercapacitors (SCs) in thin and flexible film are attracting increasing attention in the field of lightweight, ultrathin energy management devices for wearable electronics due to their higher power density and long cycle life.[7−9] However, the supercapacitors, storing charge in the electrochemical double layers, can only achieve relatively low energy density compared to batteries, which limits their further applications.[10] The high surface area allows the storage of large amounts of charge in the double layers for a given weight of the device, which results in both high energy and power density. Consequently, numerous studies have been focused on introducing new material systems with very high surface area, which provides extensive interfaces between the electrode and electrolyte.[11−15] Recently, some exciting work claimed that the energy densities of graphene-based electrodes for supercapacitors approached or even exceeded that of batteries.[16−19] However, the actual device performance of these works may be rather mediocre, because the device includes not only active materials but also electrolyte, binder, separator, current collectors, and packaging.[20] The energy density (E_{stack}) based on the whole supercapacitor stack, including two electrodes, electrolyte, a separator between the two electrodes, and current collectors (substrates), was recently recommended to be a more reliable parameter than that based on two electrodes ($E_{electrode}$) to evaluate the real potential of a material for supercapacitors.[21,22] E_{stack} is related to the

* Address correspondence to kangjianli@tjpu.edu.cn, nqzhao@tju.edu.cn.

Received for review October 4, 2014 and accepted January 7, 2015.

Published online January 07, 2015
10.1021/nn505658u

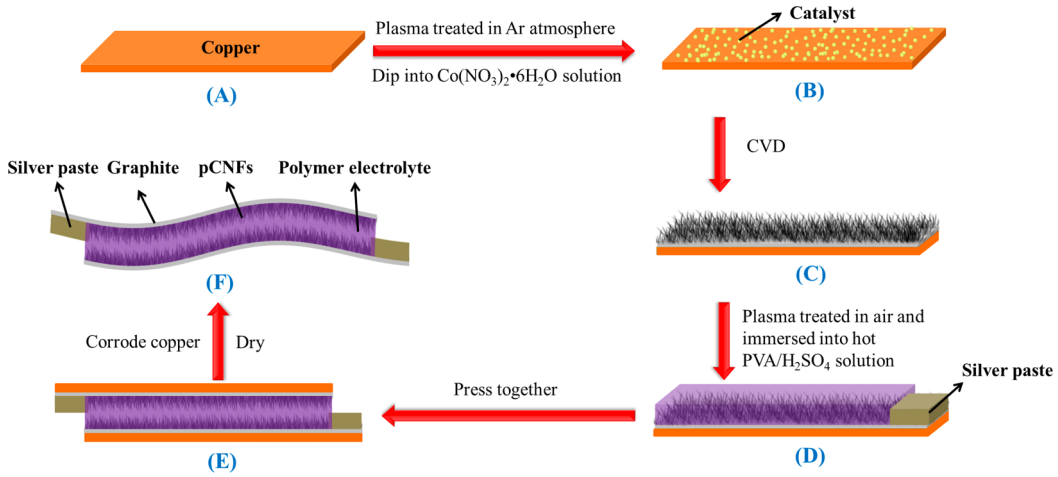

Figure 1. Schematic diagram of the fabrication process of the flexible solid-state supercapacitors based on pCNFs/G hybrid films.

specific capacitance of the active component in a single electrode (C, F g^{-1}), nominal voltage (U, V) of the supercapacitor, and fraction of the electrodes in the device stack ($f_{electrode}$, %) as follows:

$$E_{electrode} = \frac{CU^2}{8}$$

$$E_{stack} = E_{electrode} f_{electrode}$$

Improvement in E_{stack} requires maximizing the values of C, U, and $f_{electrode}$. However, increasing $f_{electrode}$ by the thickness of the electrodes, especially for pseudocapacitors, is difficult without substantially compromising the C and/or cycle life. To address this, three-dimensional current collectors (nanoporous metal) were recently introduced, which obviously improved the volumetric performance of the device.[23,24] However, the gravimetric performance of these devices seems uncompelling due to the low loading mass of active materials in the nanoporous metals. Although macroporous graphene-based electrodes show attractive gravimetric performance, their volumetric energy density is far from satisfactory due to the large empty space in the electrodes.[25,26] In some cases, especially for the thin-film SCs, the gravimetric energy density is almost irrelevant compared to the areal or volumetric one because the weight of the active materials used in a micrometer-thin film on a chip is negligible.[20]

Herein, we assembled a micrometer-thin film SC with ultrahigh device-stack performance using two pieces of porous carbon nanofibers/ultrathin graphite (pCNFs/G) hybrid films, which were one-step synthesized by chemical vapor deposition (CVD) using a copper foil supported Co catalyst (Figure 1A–C). In the growth mechanism of the pCNFs/hybrid it was assumed that Co nanoparticles catalyzed the pCNF growth while the underneath Cu foil decomposed the hydrocarbon feedback simultaneously to form a graphite layer. The *in situ* formation of a CNF–graphite heterojunction produced a seamless and ohmic contact, similar to that of the CNT–graphene hybrid synthesized by CVD.[27,28] The resulting free-standing pCNFs/G film, with an areal density of 0.75 mg cm^{-2} after removing the Cu foil and catalyst, was directly used as an electrode in the SC without any addition of either binder or metal-based current collector. The ultrathin and continuous graphite sheet (~25 nm) is mechanically compliant to support the pCNFs even after etching the copper substrate and thus can work as both current collector and support with nearly ignorable fraction in the SC stack, compared to the active materials (pCNFs). The large specific surface area of the pCNFs/G hybrid (~352 m^2 g^{-1}) mainly originates from the mesoporous surface in the pCNFs, resulting in fully accessible channels for ion transport. Consequently, the accumulated electrons can be duly transported from the pCNFs to graphite (current collectors) due to the ohmic contact at their junction, and the solid-state SCs, assembled by gelled electrolyte sandwiching between two pieces of pCNFs/G (Figure 1D–F), exhibit ultrahigh energy density (2.4 mWh cm^{-3}) and power density (23 W cm^{-3}) based on the whole device stack.

RESULTS AND DISCUSSION

Figure 2A displays the optical images of the free-standing pCNFs/G hybrid film after removing the copper foil. It can be seen that the film is highly flexible and robust. The scanning electron microscopy (SEM) image indicates that pCNF networks with a thickness of ~10 μm were seamlessly grown on an ultrathin graphite sheet (~25 nm) (Figure 2B). Viewing the high-magnification SEM (Figure 2C and D) and TEM images (Figure 2E) reveals that the as-prepared CNFs with an average diameter of ~80 nm exhibit mesoporous structure, ranging from 2 nm to over 10 nm. Moreover, the underneath graphite sheet also is mesoporous

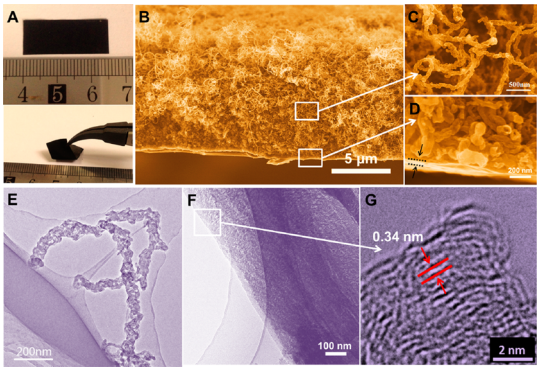

Figure 2. (A) Photograph of a pCNFs/G hybrid film, demonstrating its integrity and flexibility. (B) Low-magnification SEM image of the microstructure of the hybrid film. (C) High-magnification SEM image of the porous CNFs and (D) the area where porous CNFs are connected with the ultrathin graphite sheet. (E) TEM image of the porous CNFs. (F) TEM and (G) high-magnification TEM images of the porous graphite sheet. The color of the images was enhanced using Photoshop software.

(Figure 2F and G). High-resolution TEM images demonstrate that the graphitic layers of the porous graphite sheet are continuous, and dangling bonds are seldom observed, although the orientation is somewhat disordered (Figure 2G), inferring the good graphitization of the porous graphite.[29,30] The porous structure of the pCNFs/G hybrid film was further confirmed by nitrogen adsorption and desorption measurements (Figure S1). A typical type-IV isotherm with a distinct adsorption hysteresis loop indicates that there is a relatively large amount of micropores and mesopores in the porous CNFs (Figure S1 A). Brunauer–Emmett–Teller (BET) and density functional theory (DFT) analyses reveal that the G/pCNFs hybrid film has a high specific surface area of ~352 m^2 g^{-1} and the pore volume (0.539 cm^3 g^{-1}) mainly lies in pore sizes of 1–10 nm, producing an ultrahigh external surface area (~305 m^2 g^{-1}) (Figure S1 B). The quality of the G/pCNFs hybrid film was further investigated by Raman spectroscopy (Figure S2). The obtained I_D/I_G value of 0.75 indicates the high graphitization of the as-prepared film, consistent with TEM observations. Combined with the large surface area with suitable pore size to allow ion transfer freely, the high-quality pCNFs/G with mesopores are promising candidates as electrodes for SCs.[30]

A symmetric solid-state SC was assembled by attaching two pieces of pCNFs/G hybrid films onto each side of a H_2SO_4–PVA gel membrane. Macroscopically, the entire device shows the superior mechanical property of flexibility, which can be twisted (middle in Figure 3A), folded (right in Figure 3A), and even rolled up without any cracking. The SEM image of a thus-assembled SC is shown in Figure 3B. The typical thickness of the entire device was ~26 μm, which is much thinner than the commercial standard A4 print paper (typically 100 μm measured by a screw micrometer).

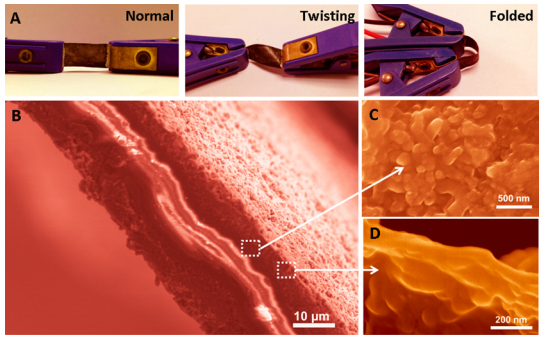

Figure 3. (A) Digital pictures of the solid-state device (size ~1 cm × 2 cm) under normal (left), twisting (middle), and folded condition (right). (B) SEM image of the cross section of the ultrathin solid-state device, which was obtained by cracking the sample in liquid nitrogen (N_2). (C, D) High-magnification SEM images of the local area in B, indicating that the porous CNFs were well bonded with the solid-state H_2SO_4–PVA gelled electrolyte. The color of the images was enhanced using Photoshop software.

To increase the wettability and active sites of pCNFs with electrolyte, the hybrid film was treated by plasma under an air atmosphere, which introduced abundant $-NO_2$, $-NH_2$, C–O, and C═O groups on the surface of the pCNFs (Figure S3, Figure S4) and improved the wettability of the pCNFs without any morphology changes observed. As a result, the pores in and gaps between pCNFs were inclined to be filled in with the polymer gelled electrolyte. High-magnification SEM images, as shown in Figure 3C,D, confirmed that the porous CNFs were fully penetrated with the gelled electrolyte, inferring that the whole pCNFs/G hybrid was well contacted with the electrolyte. The fast ion/electron transport in the electrodes was further confirmed by electrochemical impedance spectroscopy (EIS), as shown in Figure S5. The series resistance of the device is estimated to be 2.1 Ω, which is very close to that measured in 1 M H_2SO_4 aqueous electrolyte (1.7 Ω), inferring the good conductivity of the gelled electrolyte and very low internal resistance of the solid-state SC.[31,32]

Cyclic voltammogram (CV) curves of the pCNTs/G hybrid at various scan rates are shown in Figure 4A and Figure S6. The rectangular shapes of the CVs, even at a high scan rate of 500 mV s^{-1}, were retained, inferring their excellent rate performance. At a scan rate of 5 mV s^{-1}, the calculated gravimetric capacitance of the electrode (including active materials and current collector) achieves 128 F g^{-1} (Figure 4B), while the specific capacitance still stays at 90 F g^{-1} at a high scan rate of 500 mV s^{-1}, which falls in the upper range of the reported capacitance values for carbon-based solid-state SCs.[33] The high rate performance of the device can be accounted for by the porous structure of the pCNFs/G hybrid and seamless bonding nature between pCNFs and G, which can effectively absorb the gelled electrolyte and minimize the diffusion resistance of the electron/ion transport. Moreover,

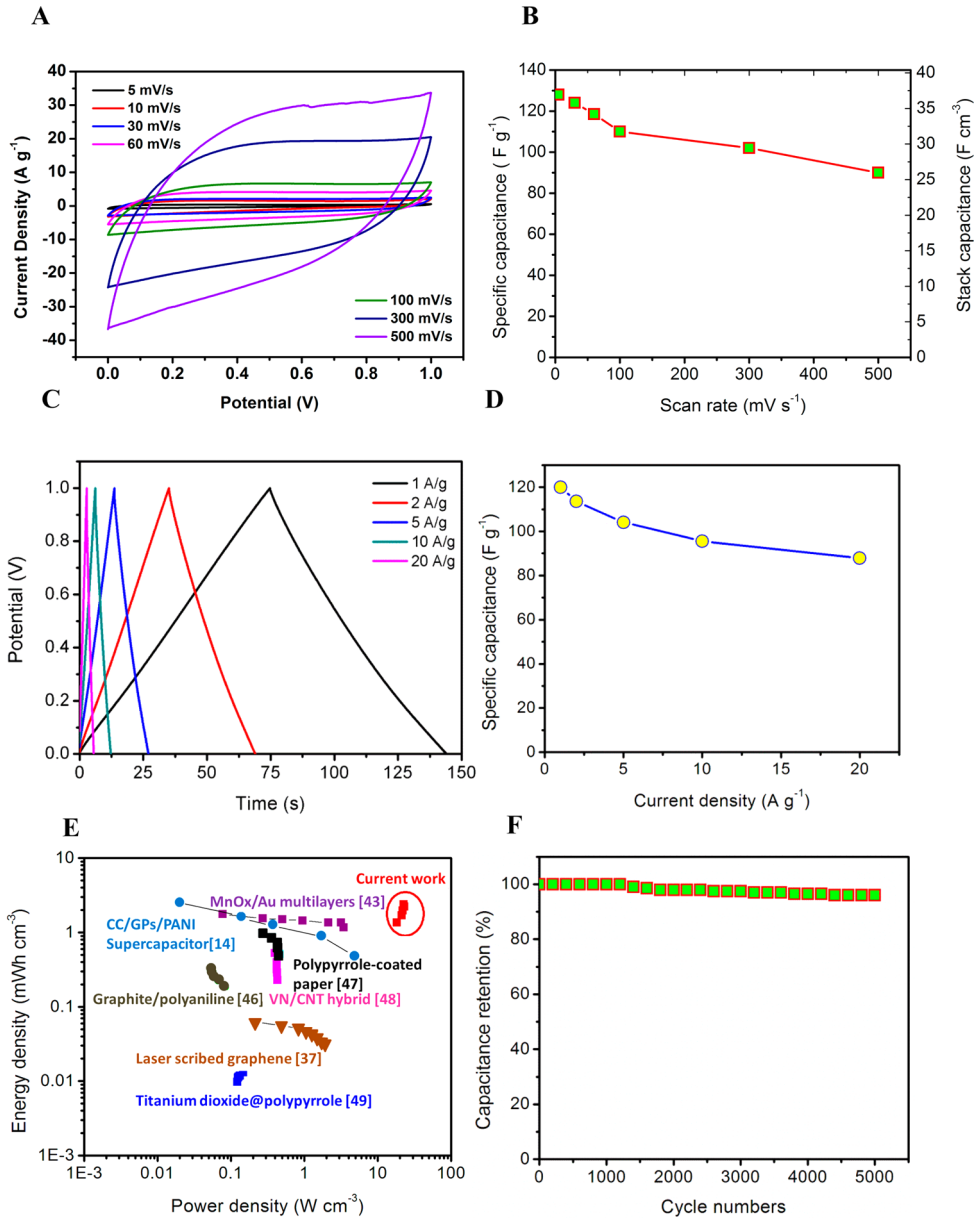

Figure 4. (A) Typical cyclic voltammograms of the flexible solid-state device at different scan rates from 30 to 500 mV s^{-1}. (B) Gravimetric specific capacitance and stack capacitances against the whole device *versus* the scan rates. (C) Galvanostatic charge/discharge curves at different current density and (D) the specific capacitances *versus* current density. (E) Energy and power density of the pCNF/G SCs with a comparison with the previously reported devices. (F) Cycling stability of the device at a current density of 5 A/g.

the plasma-treated doping of the p-CNFs by oxygen and nitrogen also contributes to the high capacitive performance of the device.[34,35] In addition, the volumetric capacitance against the whole device stack is calculated to be ~37 F cm^{-3} (~96 F cm^{-3} for a single electrode) (Figure 4B), which is an order of magnitude higher than that of the graphene-based SCs[36−38] and even higher than that of the pseudocapacitive solid-state thin SCs.[39−43] It is more interesting that the gravimetric $f_{electrode}$ in this device reaches up to 26%. Thus, the gravimetric specific capacitance of the whole device (~33 F g^{-1}) is also competitive for commercial applications.

To further investigate the capacitive performance of the G/pCNFs hybrid, the charge/discharge behavior of the solid-state device was examined by its responses in the voltage range between 0 and 1 V at various current densities (Figure 4C). The largest specific capacitance of the G/pCNFs per one electrode mass is ~120 F g^{-1} at a current density of 1 A g^{-1} (Figure 4D), which is substantially higher than those of the previously reported CNT-based solid-state devices (50−115 F g^{-1} at 1 A g^{-1}).[44,45] When the current density is increased from 1 A/g to 20 A/g, the solid-state device exhibits a higher rate performance (~88 F g^{-1} at 20 A g^{-1}, 73% retention, Figure 4D), consistent with the CV results.

The volumetric power and energy densities against the device stack, as well as a more comprehensive comparison with the previously reported devices, are plotted in the Ragone plot in Figure 4E and listed in Table S1. The maximum energy density is up to 2.4 mWh cm^{-3} (6.24 μWh cm^{-2}), which is orders higher than that of most recently reported electric double-layer capacitors and pseudocapacitors.[37,46−49] The maximum volumetric power density is 23 W cm^{-3} (59.8 mW cm^{-2}), which is almost 1 order of magnitude higher than that of CC/GPs/NANI[14] and MnO_X/Au multilayers[43] and laser-scribed graphene-based SCs,[37] 2 orders of magnitude higher than that of polypyrrole-coated paper,[47] VN/CNT hybrid,[48] and titanium dioxide@polypyrrole-based SCs,[49] and 3 orders of magnitude higher than that of graphite/polyaniline[46]-based SCs.

Designed for ultrathin wearable devices, we further evaluated their flexibility under various bending angles. Interestingly, the CV curves obtained at various bending angles show nearly the same capacitive behavior (Figure S7), displaying excellent capacitance stability at different bending curvatures. To demonstrate the application prospect for these materials, we assembled three SCs in series, and after charging at 3 V, the device could power a light-emitting diode (LED) as shown in Figure S8.

The cyclic stability of the device was explored by a charge/discharge test at a current density of 5 A g^{-1}. After 5000 cycles, the capacitance still remained at 96% of the initial capacitance, demonstrating excellent long-term performance durability (Figure 4F). Even in a bending state, the device shows similar behavior, which is attributed to the high mechanical flexibility of the electrodes along with the interpenetrating network structure between the pCNFs/G electrodes and the gelled electrolyte. In order to comprehensively evaluate the performance of the as-prepared SCs, a radar plot summarizing the performance in this work and in the literature was drawn, Figure S9. The larger area encompassed within a radar plot further indicated the better overall performance of the p-CNFs/G-based SCs than that in the litetature.[9]

CONCLUSION

In summary, a flexible, solid-state supercapacitor was designed and fabricated with a total thickness of ~26 μm, using two pieces of novel pCNFs/G hybrid films as electrodes and H_2SO_4−PVA gel as solid-state electrolyte. The symmetric SC thus produced offers ultrahigh energy density (2.4 mWh cm^{-3}) and power density (23 W cm^{-3}) based on the device stack and exhibits almost identical performance at various curvatures, which suggests its wide application potential in powering wearable/miniaturized electronics. Moreover, the performance of the device will be further improved by depositing high-performance pseudocapacitive materials (such as conducting polymers or transition metal oxides) on the pCNFs or constructing an asymmetric SC model where the voltage range would be greatly expanded.

EXPERIMENTAL SECTION

Synthesis of the pCNFs/G Hybrid Structure. pCNFs/G were synthesized by CVD using a Co catalyst supported on copper foil with a thickness of 25 μm (Alfa Aesar). The copper foil was pretreated by plasma in an Ar atmosphere, and the pretreatment voltage and current were 50 V and 2A, respectively. A Co catalyst precursor, supported on copper foil, was prepared by a dip-coating technique using $Co(NO_3)_2 \cdot 6H_2O$ (0.01 mol L^{-1}) solution. The supported Co catalyst precursor was transferred into the horizontal tube furnace and calcined at 400 °C for 1 h in an Ar atmosphere. Then, the furnace was directly heated to the reaction temperature under Ar flow. The pCNFs/G growth was performed at 800 °C with a mixture of C_2H_2 (10 sccm), Ar (400 sccm), and H_2 (100 sccm) for 10 min. Finally, the furnace was cooled to room temperature under the protection of argon gas (100 sccm). To increase the wettability and active sites of pCNFs with an electrolyte, the hybrid film was treated by plasma for 1 min under an air atmosphere. The pretreatment voltage and current were 70 V and 0.5 A.

Assembly of the Flexible Solid-State Supercapacitors. First, 6 g of H_2SO_4 was mixed with 60 mL of deionized water, and then 6 g of polyvinyl alcohol (PVA) powder was added. The whole mixture was heated steadily up to 85 °C under vigorous stirring until the solution became clear. Then the solution was kept at 85 °C without stirring. Second, two pieces of the obtained pCNFs/G, grown on copper foil, were treated by plasma under an air atmosphere, immersed in the hot solution for 2 min, and then picked out. After that, the electrode with a thin solution coating layer was left in the fume hood at room temperature for 4 h to vaporize the excess water. Then the two pieces of electrode were pressed together under a pressure of 1 MPa for 30 min by a sheeting presser to assemble a supercapacitor. The electrolyte was solidified and functioned as a glue that held all the device components together, improving the mechanical integrity. Third, the assembled device was immersed into a methanol solution of ferric chloride (1 mol L^{-1}) for 24 h to corrode the copper foil. Then the final device without the copper substrate was immersed into the mixture solution (6 g of H_2SO_4 + 60 mL of methanol) for 24 h to remove the residual ferric chloride. Finally, the solid-state SC was left in the fume hood at room temperature for 2 h to dry.

Characterization. The structure of the pCNFs/G was characterized by scanning electron microscopy (SEM, Hitachi S4800) and transmitting electron microscopy (TEM, Philps Tecnai G2 F20). A micro-Raman spectrometer (Renishaw, In*Via* microscope) with a 532 nm laser was used in the Raman study. The CV, galvanostatic charge/discharge, and EIS with frequency ranging from 0.01 Hz to100 kHz were conducted with an electrochemical station (CHI 660D). Nitrogen adsorption isotherms of G/pCNFs were measured at 77 K using an Autosorb iQ instrument (Quantachrome U.S.). The total surface area was calculated with the BET method, and the pore size distribution data were calculated using the DFT method based on the adsorption and desorption data. The functional group on the surface of the G/pCNFs was characterized by FT-IR (Thermo Scientific Nicolet 6700) and X-ray photoelectron spectroscopy (XPS, Axis Ultra DLD) with an Al Kα (mono) anode at an energy of 120 W in a vacuum of 5×10^{-9} Torr.

Conflict of Interest: The authors declare no competing financial interest.

Acknowledgment. This work is sponsored by the National Natural Science Foundation of China (Nos. 51001080, 51272173,

51472177), Tianjin Research Program of Application Foundation and Advanced Technology (Nos. 14JCYBJC20900, 14JCYBJC19600, 12ZCZDGX00800), and Program for Changjiang Scholars and Innovative Research Team in University (PCSIRT) of the Ministry of Education of China (No. IRT13084).

Supporting Information Available: Raman, BET, IR, and XPS analysis of the prepared pCNFs/G hybrid film; Nyquist plots, radar plots, and LED lighting demonstration of the flexible solid-state device; electrochemical performance of the device under bending. This material is available free of charge *via* the Internet at http://pubs.acs.org.

REFERENCES AND NOTES

1. Wang, K.; Zhao, P.; Zhou, X. M.; Wu, H. P.; Wei, Z. X. Flexible Supercapacitors Based on Cloth-Supported Electrodes of Conducting Polymer Nanowire Array/SWCNT Composites. *J. Mater. Chem.* **2011**, *21*, 16373–16378.
2. Tarascon, J. M.; Armand, M. Issues and Challenges Facing Rechargeable Lithium Batteries. *Nature* **2001**, *414*, 359–367.
3. Meng, C. Z.; Liu, C. H.; Chen, L. Z.; Hu, C. H.; Fan, S. S. Highly Flexible and All-Solid-State Paperlike Polymer Supercapacitors. *Nano Lett.* **2010**, *10*, 4025–4031.
4. Yan, C.; Lee, P. S. Stretchable Energy Storage and Conversion Devices. *Small* **2014**, 10.1002/smll.201302806.
5. Beidaghi, M.; Gogotsi, Y. Capacitive Energy Storage in Micro-Scale Devices: Recent Advances in Design and Fabrication of Micro-Supercapacitors. *Energy Environ. Sci.* **2014**, *7*, 867–884.
6. Jost, K.; Dion, G.; Gogotsi, Y. Textile Energy Storage in Perspective. *J. Mater. Chem. A* **2014**, *2*, 10776–10787.
7. Miller, J. R.; Simon, P. Electrochemical Capacitors for Energy Management. *Sci. Mag.* **2008**, *321*, 651–652.
8. Liu, C.; Li, F.; Ma, L. P.; Cheng, H. M. Advanced Materials for Energy Storage. *Adv. Mater.* **2010**, *22*, E28–E62.
9. Xiong, G.; Meng, C.; Reifenberger, R.; Irazoqui, P.; Fisher, T. A Review of Graphene-Based Electrochemical Microsupercapacitors. *Electroanalysis* **2014**, *26*, 30–51.
10. Liu, R.; Duay, J.; Lee, S. B. Heterogeneous Nanostructured Electrode Materials for Electrochemical Energy Storage. *Chem. Commun.* **2011**, *47*, 1384–1404.
11. Huang, Y.; Liang, J.; Chen, Y. An Overview of the Applications of Graphene-Based Materials in Supercapacitors. *Small* **2012**, *8*, 1805–1832.
12. Xiong, G.; Hembram, K.; Reifenberger, R.; Fisher, T. MnO_2-Coated Graphitic Petals for Supercapacitor Electrodes. *J. Power Sources* **2013**, *227*, 254–259.
13. Xiong, G.; Hembram, K.; Zakharow, D.; Reifenberger, R.; Fisher, T. Controlled Thin Graphitic Petal Growth on Oxidized Silicon. *Diamond Relat. Mater.* **2012**, *27–28*, 1–9.
14. Xiong, G.; Meng, C.; Reifenberger, R.; Irazoqui, P.; Fisher, T. Graphitic Petal Electrodes for All-Solid-State Flexible Supercapacitors. *Adv. Energy Mater.* **2014**, *4*, 1300515.
15. Dai, L.; Chang, D. W.; Baek, J. B.; Lu, W. Carbon Nanomaterials for Advanced Energy Conversion and Storage. *Small* **2012**, *8*, 1130–1166.
16. Liu, C.; Yu, Z.; Neff, D.; Zhamu, A.; Jang, B. Z. Graphene-Based Supercapacitor with an Ultrahigh Energy Density. *Nano Lett.* **2010**, *10*, 4863–4868.
17. Cheng, Q.; Tang, J.; Ma, J.; Zhang, H.; Shinya, N.; Qin, L. C. Graphene and Carbon Nanotube Composite Electrodes for Supercapacitors with Ultra-High Energy Density. *Phys. Chem. Chem. Phys.* **2011**, *13*, 17615–17624.
18. Zhang, F.; Zhang, T.; Yang, X.; Zhang, L.; Leng, K.; Huang, Y.; Chen, Y. A High-Performance Supercapacitor-Battery Hybrid Energy Storage Device Based on Graphene-Enhanced Electrode Materials with Ultrahigh Energy Density. *Energy Environ. Sci.* **2013**, *6*, 1623–1632.
19. Bo, Z.; Zhu, W.; Ma, W.; Wen, Z.; Shuai, X.; Chen, J.; Yan, J.; Wang, Z.; Cen, K.; Feng, X. Vertically Oriented Graphene Bridging Active-Layer/Current-Collector Interface for Ultrahigh Rate Supercapacitors. *Adv. Mater.* **2013**, *25*, 5799–5806.
20. Gogotsi, Y.; Simon, P. True Performance Metrics in Electrochemical Energy Storage. *Science* **2011**, *334*, 917–918.
21. Kim, T. Y.; Jung, G.; Yoo, S.; Suh, K. S.; Ruoff, R. S. Activated Graphene-Based Carbons as Supercapacitor Electrodes with Macro- and Mesopores. *ACS Nano* **2013**, *7*, 6899–6905.
22. Yang, X.; Cheng, C.; Wang, Y.; Qiu, L.; Li, D. Liquid-Mediated Dense Integration of Graphene Materials for Compact Capacitive Energy Storage. *Science* **2013**, *341*, 534–537.
23. Lang, X.; Hirata, A.; Fujita, T.; Chen, M. Nanoporous Metal/Oxide Hybrid Electrodes for Electrochemical Supercapacitors. *Nat. Nanotechnol.* **2011**, *6*, 232–236.
24. Kang, J. L.; Hirata, A.; Qiu, H.-J.; Chen, L. Y.; Ge, X. B.; Fujita, T.; Chen, M. W. Self-Grown Oxy-Hydroxide@Nanoporous Metal Electrode for High-Performance Supercapacitors. *Adv. Mater.* **2014**, *26*, 269–272.
25. Xu, Y. X.; Lin, Z. Y.; Huang, X. Q.; Liu, Y.; Huang, Y.; Duan, X. F. Flexible Solid-State Supercapacitors Based on Three-Dimensional Graphene Hydrogel Films. *ACS Nano* **2013**, *7*, 4042–4049.
26. Cao, X.; Yin, Z.; Zhang, H. Three-Dimensional Graphene Materials: Preparation, Structures and Application in Supercapacitors. *Energy Environ. Sci.* **2014**, *7*, 1850–1865.
27. Das, S.; Seelaboyina, R.; Verma, V.; Lahiri, I.; Hwang, J. Y.; Banerjee, R.; Choi, W. Synthesis and Characterization of Self-Organized Multilayered Graphene-Carbon Nanotube Hybrid Films. *J. Mater. Chem.* **2011**, *21*, 7289–7295.
28. Zhu, Y.; Li, L.; Zhang, C.; Casillas, G.; Sun, Z.; Yan, Z.; Ruan, G.; Peng, Z.; Raji, A. O.; Kittrell, C.; Hauge, R. H.; Tour, J. M. A Seamless Three-Dimensional Carbon Nanotube Graphene Hybrid Material. *Nat. Commun.* **2012**, *2*, 1225–1227.
29. Kang, J. L.; Qin, K. Q.; Zhang, H.; Hirata, A.; Wang, J. Q.; Chen, M. W.; Zhao, N. Q.; Sun, R. L.; Fujita, T.; Shi, C. S.; Qiao, Z. J. Direct Synthesis of Fullerene-Intercalated Porous Carbon Nanofibers by Chemical Vapor Deposition. *Carbon* **2012**, *50*, 5162–5166.
30. Ji, L.; Zhang, X. Fabrication of Porous Carbon Nanofibers and Their Application as Anode Materials for Rechargeable Lithium-Ion Batteries. *Nanotechnology* **2009**, *20*, 155705.
31. Taberna, P. L.; Simon, P.; Fauvarque, J. F. Electrochemical Characteristics and Impedance Spectroscopy Studies of Carbon-Carbon Supercapacitors. *J. Electrochem. Soc.* **2003**, *150*, A292–A300.
32. Pech, D.; Brunet, M.; Durou, H.; Huang, P.; Mochalin, V.; Gogotsi, Y.; Taberna, P.; Simon, P. Ultrahigh-Power Micrometre-Sized Supercapacitors Based on Onion-like Carbon. *Nat. Nanotechnol.* **2010**, *5*, 651–654.
33. Wang, G.; Wang, H.; Lu, X.; Ling, Y.; Yu, M.; Zhai, T.; Tong, Y.; Li, Y. Solid-State Supercapacitor Based on Activated Carbon Cloths Exhibits Excellent Rate Capability. *Adv. Mater.* **2014**, *26*, 2676–2682.
34. Wei, J.; Zhou, D.; Sun, Z.; Deng, Y.; Xia, Y.; Zhao, D. A Controllable Synthesis of Rich Nitrogen-Doped Ordered Mesoporous Carbon for CO_2 Capture and Supercapacitors. *Adv. Funct. Mater.* **2013**, *23*, 2322–2328.
35. Chen, P.; Yang, J.; Li, S.; Wang, Z.; Xiao, T.; Qian, Y.; Yu, S. Hydrothermal Synthesis of Macroscopic Nitrogen-Soped Graphene Hydrogels for Ultrafast Supercapacitor. *Nano Energy* **2013**, *2*, 249–256.
36. Miller, J. R.; Outlaw, R. A.; Holloway, B. C. Graphene Double-Layer Capacitor with ac Line-Filtering Performance. *Science* **2010**, *329*, 1637–1639.
37. Pech, D.; Brunet, M.; Durous, H.; Huang, P.; Mochalin, V.; Gogotsi, Y.; Taberna, P.; Simon, P. Ultrahigh-Power Micrometre-Sized Supercapacitors Based on Onion-Like Carbon. *Nat. Nanotechnol.* **2010**, *5*, 651.
38. Ren, G.; Pan, X.; Bayne, S.; Fan, Z. Kilohertz Ultrafast Electrochemical Supercapacitors Based on Perpendicularly-Oriented Graphene Grown Inside of Nickel Foam. *Carbon* **2014**, *71*, 94–101.
39. Wu, Z. S.; Parvez, K.; Feng, X.; Müllen, K. Graphene-Based in-Plane Micro-Supercapacitors with High Power and Energy Densities. *Nat. Commun.* **2013**, *4*, 2487–2490.
40. Xiao, X.; Peng, X.; Jin, H.; Li, T.; Zhang, C.; Gao, B.; Hu, B.; Huo, K.; Zhou, J. Freestanding Mesoporous VN/CNT Hybrid

Electrodes for Flexible All-Solid-State Supercapacitors. *Adv. Mater.* **2013**, *25*, 5091–5097.
41. Yang, L.; Yao, B.; Hu, B.; Huo, K.; Chen, W.; Zhou, J. Polypyrrole-Coated Paper for Flexible Solid-State Energy Storage. *Energy Environ. Sci.* **2013**, *6*, 470–476.
42. Meng, F.; Ding, Y. Sub-Micrometer-Thick All-Solid-State Supercapacitors with High Power and Energy Densities. *Adv. Mater.* **2011**, *23*, 4098–4102.
43. Si, W.; Yan, C.; Chen, Y.; Oswald, S.; Han, L.; Schmidt, O. G. On Chip, All Solid-State and Flexible Micro-Supercapacitors with High Performance Based on MnOx/Au Multilayers. *Energy Environ. Sci.* **2013**, *6*, 3218–3223.
44. Hu, S.; Rajamani, R.; Yu, X. Flexible Solid-State Paper Based Carbon Nanotube Supercapacitor. *Appl. Phys. Lett.* **2012**, *100*, 104103.
45. Kaempgen, M.; Chan, C. K.; Ma, J.; Cui, Y.; Gruner, G. Printable Thin Film Supercapacitors Using Single-Walled Carbon Nanotubes. *Nano Lett.* **2009**, *9*, 1872–1876.
46. Yao, B.; Yuan, L.; Xiao, X.; Zhang, J.; Qi, Y.; Zhou, J.; Zhou, J.; Hu, B.; Chen, W. Paper-Based Solid-State Supercapacitors with Pencil-Drawing Graphite/Polyaniline Networks Hybrid Electrodes. *Nano Energy* **2013**, *2*, 1071–1078.
47. Yuan, L.; Yao, B.; Hu, B.; Huo, K.; Chen, W.; Zhou, J. Polypyrrole-Coated Paper for Flexible Solid-State Energy Storage. *Energy Environ. Sci.* **2013**, *6*, 470–476.
48. Xiao, X.; Peng, X.; Jin, H.; Li, T.; Zhang, C.; Gao, B.; Hu, B.; Huo, K.; Zhou, J. Freestanding Mesoporous VN/CNT Hybrid Electrodes for Flexible All-Solid-State Supercapacitors. *Adv. Mater.* **2013**, *25*, 5091–5097.
49. Yu, M.; Zeng, Y.; Zhang, C.; Lu, X.; Lu, X.; Zeng, C.; Yao, C.; Yang, Y.; Tong, Y. Titanium Dioxide@Polypyrrole Core–Shell Nanowires for All Solid-State Flexible Supercapacitors. *Nanoscale* **2013**, *5*, 10806–10810.